

# Light meson radial Regge trajectories

A.M. Badalian,<sup>1</sup> B.L.G. Bakker,<sup>2</sup> and Yu.A. Simonov<sup>3,1</sup>

<sup>1</sup>*State Research Center,*

*Institute of Theoretical and Experimental Physics, Moscow, Russia*

<sup>2</sup>*Department of Physics and Astronomy, Vrije Universiteit, Amsterdam*

<sup>3</sup>*Jefferson Laboratory, Newport News, VA 23606, USA*

## Abstract

A new physical mechanism is suggested to explain the universal depletion of high meson excitations. It takes into account the appearance of holes inside the string world sheet due to  $q\bar{q}$  pair creation when the length of the string exceeds the critical value  $R_1 \simeq 1.4$  fm. It is argued that a delicate balance between large  $N_c$  loop suppression and a favorable gain in the action, produced by holes, creates a new metastable (predecay) stage with a renormalized string tension which now depends on the separation  $r$ . This results in smaller values of the slope of the radial Regge trajectories, in good agreement with the analysis of experimental data in Refs. [3].

## I. INTRODUCTION

Recently a number of radially excited mesons have been experimentally observed [1]-[4] and it was discovered that for excitations like  $a_J(2P)$ ,  $\omega_3(2D)$ , and  $\rho(2D)$  their masses are 100-200 MeV lower than the theoretical predictions in different models, in particular in the relativized potential model (RPM)[5] and in the flux tube model [6]. A  $K$ -matrix analysis of the Crystal Barrel data has shown that the Regge trajectories as a function of the radial quantum number  $n_r$  continue to be linear up to high excitations like the four  $L$  states ( $n_r = 0, 1, 2, 3$ ) and can be described by the  $n_r$ -trajectory (the radial Regge trajectory) [3]:

$$M^2(n_r, L) = M^2(0, L) + \Omega_L n_r \quad (\text{fixed } L) \quad (1.1)$$

where the slope  $\Omega_L$  was found to vary in the narrow range  $1.15 \leq \Omega \leq 1.30 \text{ GeV}^2$  for different  $L$ -wave states.

In Ref. [7] the orbital excitations of the light mesons ( $n_r = 0, L \leq 5$ ) were studied in detail in the framework of the QCD string approach[8] and the spin-averaged meson masses  $\bar{M}(nL)$ , the Regge slope  $\alpha'_L$ , and the intercept  $\alpha_L(0)$  were calculated analytically and expressed through a single parameter, the string tension  $\sigma$ , while the Regge intercept  $\alpha_L(0)$  does not depend on  $\sigma$  and is a universal number. The calculated values of  $\bar{M}(nL)$ ,  $\alpha'_L$ , and  $\alpha_L(0)$  turn out to be in very good agreement with the experimental data. (Note our notation: a state denoted by  $nL$  has radial quantum number  $n_r = n - 1$ , so the lowest state with a given angular momentum  $L$  is  $1L$  and has  $n_r = 0$ .)

The situation appears to be different for the radial excitations (called also *radials* in what follows) calculated also for the linear string potential (or the linear plus Coulomb potential) with the same string tension. Thus the masses of the radials obtained do lie on a linear trajectory Eq. (1.1) which has a slope that is practically independent of  $L$ , but its value  $\Omega_0 \simeq 2.0 \text{ GeV}^2$  appears to be a factor 1.6 - 1.5 larger than  $\Omega(\text{exp})$ , the value extracted from the experimental data [3] (see Sect. 2). In particular, the masses of the second radial excitations (and even some first ones like  $2D$  and  $2F$ ) are 100-150 MeV ( $n_r = 2$ ) (50 - 100 MeV for  $n_r = 1$ ) higher than  $M(\text{exp})$  from Refs. [1] - [4].

This phenomenon, the lowering of the masses of the radials, was already discussed in Refs. [9] and [10] where it was supposed that this effect is connected with the opening of new channels, i.e. with hadronic shifts. However, hadronic shifts cannot produce the

global, quantum-number independent shift down of all radials on the  $n_r$ -trajectory having been observed in experiment. In particular it cannot provide almost the same slope  $\Omega$  in Eq. (1.1) for different  $L$ , since hadronic shifts strongly depend on the quantum numbers of a decay channel, the closeness to the decay thresholds, the widths, and many other specific features of meson decays [11].

Thus a basic paradox of mesonic spectra is that there are highly excited meson states with large width, implying strong coupling to decay channels, which nevertheless lie on linear Regge trajectories. This situation implies that first, the string between a quark and an antiquark continues to exist up to large energy excitations and can be as large as 2.5–2.8 fm (see below). Secondly, quark pair creation does not dominate for such excitations, in particular the probability of string breaking is not large. How to reconcile these conclusions with strong decays (large width) of the Regge-string mesons? One can argue that pair creation is suppressed as  $1/N_c$  at large  $N_c$ . Moreover, in experiment this parameter appears to be 1/10 rather than 1/3 for  $N_c = 3$  which can be seen in the width to mass ratio for large excitations. The present paper suggests at least a partial answer to these questions taking as a characteristic example the radially excited mesons and generalizing to all highly excited light mesons which serve as a good illustration to the paradox stated above.

So, to explain the “global correlated shift down” of the radial excitations we suggest here an alternative physical picture, which in first turn takes into account the behavior of the string in highly excited hadrons, and in addition the specific character of the  $\pi$ -meson interaction with a light quark (antiquark) and the string connecting them.

In contrast to hadronic decays like  $\rho - \rho$ ,  $\rho - a_0$ ,  $\omega - \omega$  etc., which may occur due to  $q\bar{q}$  loop creation inside the string’s world sheet and subsequent string breaking, the  $\pi$ -meson, as well as other Goldstone particles, locally interacts with a quark (antiquark) sitting at the end of the string [12] and therefore the string may not break due to the emission of a  $\pi$ -meson from a quark.

The same statement is true when the creation of a  $\pi$ -meson is accompanied by a  $\rho$ ,  $a_0$  or  $f_0$  meson, since these mesons are actually described by the remaining string in the final state. Therefore it is natural to assume that below the threshold of  $\rho - \rho$ , ( $\omega - \omega$  etc.), i.e.

$$E_{\text{thr}} \simeq 2M_\rho \pm \Gamma_\rho \geq 1.4 \text{ GeV} \quad (1.2)$$

the string effectively stays intact. When only channels like  $(n\pi)\pi$ ,  $(n\pi)\eta$ ,  $\pi - \rho$ ,  $\eta - \rho$  etc.

are open, we argue that the string between a light quark and antiquark is not modified by open channels and has the same string tension  $\sigma_0 \simeq 0.18 \text{ GeV}^2$  as the string between a static quark  $Q$  and antiquark  $\bar{Q}$ . Then one can determine the characteristic size of the string  $R_1$  which corresponds to the value  $E_{\text{thr}} \sim 1.4 \text{ GeV}$ :

$$\sigma_0 R_1 \simeq E_{\text{thr}}, \text{ or } R_1 \geq 1.4 \text{ GeV}/\sigma_0 = 1.45 \text{ fm}. \quad (1.3)$$

Thus our first assumption here is that up to distances  $\simeq 1.4 \text{ fm}$  the string potential is not distorted by meson decays. This statement is in agreement with lattice calculations where in the presence of dynamical fermions the static potential appears to be the same as in the quenched approximation up to the separations of order  $1.2 - 1.5 \text{ fm}$  [13], [14].

For higher excitations,  $E^* \geq E_{\text{thr}}$ , the  $q\bar{q}$  pair creation inside the world sheet (with the quantum numbers  ${}^3S_1$  and  ${}^3P_0$ ) is already possible and at first sight the problem is becoming essentially a two- or many-channel problem. However, we shall assume and argue here (see Section III) that up to very high excitations,  $E_{\text{cr}} \geq 2.5 \text{ GeV}$ , i.e. in the range

$$1.4 \text{ GeV} \leq E^* \leq E_{\text{cr}} \sim 2.5 \text{ GeV} \quad (1.4)$$

and for the time extensions  $\delta T \sim 1/\Gamma \leq 1.0 \text{ fm}$ , only virtual loops or loops of small sizes are created. As a result the probability of hadronic decays like  $M \rightarrow \rho - \rho$ ,  $\omega - \omega$ , is small while with a large probability the string remains unbroken. This assumption is necessary to explain the linear character of the  $n_r$ -trajectories Eq. (1.1) up to high excitations of the order of  $2.5 \text{ GeV}$ .

However, in the presence of such virtual or small  $q\bar{q}$  loops the string tension is renormalized and becomes dependent on the separation  $r$ . In the suggested picture (when at small  $r$ ,  $r \leq R_1$ ,  $\sigma = \text{constant} = \sigma_0$ ) the attenuation of the string tension is being felt only at distances  $r \geq R_1$  and continues at least up to the value,  $R_2 \sim 2.5 \text{ fm}$  with  $\sigma(R_2) = \sigma_2$ . It is important that this ‘‘asymptotic’’ value  $\sigma_2$  strongly affects the slope  $\Omega$  of the  $n_r$ -trajectory given in Eq. (1.1).

The most important feature of this picture is the existence of a prehadronization stage in the range of string parameters,

$$R_1 \sim 1.4 \text{ fm} \leq r \leq R_2 \sim 2.5 \text{ fm}, \quad T \leq T_{\text{cr}} \sim 1.0 \text{ fm}, \quad (1.5)$$

where the string tension depends on  $r$  while at the same time the string with large probability remains unbroken. The dynamics in this prehadronization region can be effectively described

in the one-channel approximation taking into account virtual quark loops and the open hadronic channels (mostly like  $(n\pi)\pi$ ,  $\pi - \rho$ ,  $\eta - \rho$  etc.) through a universal dependence of the string tension on  $r$ :

$$\begin{aligned} \sigma &= \text{constant} = \sigma_0, & r \leq R_1, \\ \sigma &= \sigma(r) & R_1 \leq r \leq R_2 \end{aligned} \tag{1.6}$$

At the present stage of the theory the function  $\sigma(r)$  is not yet calculated in full QCD and therefore we formulate here the problem in a different way: how to extract information about  $\sigma(r)$ , or the string breaking, from highly excited meson masses, in particular from the slope of the radial Regge trajectories.

We shall show here that there exists a direct connection between the slope  $\Omega$  and the two most important features of  $\sigma(r)$ : the value of  $R_1$  where the string tension is becoming  $r$ -dependent, and the value  $\sigma_2$  which characterizes the string tension in the region where breaking is already possible. In lattice calculations a flattening of the static potential due to  $q\bar{q}$  pair creation at  $r \sim 1.2 - 1.5$  fm seems to be observed [14], unfortunately, lattice points have very large errors and at present definite conclusions about the exact value and form of the static potential at large  $r$  cannot be derived from lattice measurements.

We concentrate below on these considerations and suggest a workable and simple model for the mesons of large size, both radial and orbital ones, which yields meson masses in good agreement with experiment. It will be shown that in the proposed picture the linear  $n_r$ -trajectories with a rather small slope,  $\Omega \simeq 1.3 \text{ GeV}^2$  ( $\simeq 1.5 \text{ GeV}^2$  for the spin averaged  $S$ -wave states) close to the experimental numbers, can be easily obtained.

The plan of the paper is as follows. In Section II the analytic formulas for the Regge slope and the intercept for the linear potential are derived and the masses will be expressed through a single scale parameter - the string tension. It will be shown that for the standard linear potential the slope  $\Omega_0$  is a factor 1.6 larger than in experiment. In Section III the effects of  $q\bar{q}$ -pair creation (unquenched situation) on the meson masses of large radii are discussed and in Section IV a modified nonperturbative potential is proposed for which the meson masses are calculated. In Section V the Regge slope and intercept of the  $n_r$ -trajectories are presented. In section VI our Conclusions and some prospectives are briefly discussed. In the Appendix the results of the detailed calculations for the meson spectra are included.

## II. THE PROBLEM OF HIGH EXCITATIONS FOR THE LINEAR POTENTIAL

In the QCD string approach the Hamiltonian is derived from QCD under definite and verifiable assumptions. First, the times and distances involved are considered to be larger than the gluonic correlation length  $T_g$ :  $r \gg T_g$  ( $T_g \simeq 0.2$  fm in lattice calculations [15]). This condition is always valid for the light mesons having large sizes  $R \geq 0.8$  fm. Secondly, the string (hybrid) excitation scale is large,  $\Delta M_{\text{str}} \geq 1$  GeV, and therefore in first approximation the meson and hybrid excitations are disconnected.

Then the spin-averaged mass  $\bar{M}(nL)$  of the light meson with arbitrary quantum numbers  $nL$  ( $L \leq 5$ ) are determined by the following mass formula [7, 8]:

$$\bar{M}(nL) = M_0(nL) + \Delta_{\text{str}}(nL) + \Delta_{\text{SE}}(nL) \quad (2.1)$$

where  $M_0$  is the eigenvalue of the unperturbed string Hamiltonian  $H_R^1$  coinciding with the spinless Salpeter equation (SSE):

$$\left(2\sqrt{\vec{p}^2 + m^2} + V(r)\right) \psi(nL) = M_0(nL)\psi(nL), \quad (2.2)$$

where  $m$  is the current quark mass taken here to be equal to zero ( $m = 0$ ). The potential  $V(r)$  contains in the general case both a perturbative part, the Coulomb interaction  $V_C(r)$ , and the nonperturbative string potential  $V_{\text{NP}}(r)$  with a string tension that is in general dependent on the separation  $r$  [7]:

$$V(r) = -\frac{4\alpha_s}{3r} + \sigma(r)r. \quad (2.3)$$

It is instructive to consider first a linear potential with  $\sigma = \text{constant} = \sigma_0$  with a mass formula that is more transparent and can be presented in analytical form. In this case the string correction was defined in [7, 16]:

$$\Delta_{\text{str}}(nL) = -\frac{\sigma_0 \langle r^{-1} \rangle L(L+1)}{8\mu_0^2(nL)} = -\frac{2\sigma_0 \langle r^{-1} \rangle L(L+1)}{M_0^2(nL)}, \quad (2.4)$$

where the following relations valid for the potential  $\sigma_0 r$  are used:

$$M_0(nL) = 4\mu_0(nL), \langle \sigma_0 r \rangle = 2\mu_0(nL). \quad (2.5)$$

The constituent mass  $\mu_0(nL)$  was derived to be the average of the quark kinetic energy operator [7],[8]:

$$\mu_0(nL) = \langle \sqrt{\vec{p}^2 + m^2} \rangle_{nL}. \quad (2.6)$$

From the definition Eq. (2.6) it is clear that  $\mu_0$  depends on the quantum numbers  $nL$  of a given state and can be expected to grow for high excitations.

An important contribution to the meson mass Eq. (2.1) comes from the nonperturbative self-energy term  $\Delta_{\text{SE}}(nL)$  calculated in Ref. [17]:

$$\Delta_{\text{SE}}(nL) = -\frac{4\sigma_0\eta(f)}{\pi\mu_0} = -\frac{16\sigma_0\eta(f)}{\pi M_0(nL)}, \quad (2.7)$$

where the parameter  $\eta(f)$  depends on the quark flavor  $f$  and can be calculated, see Ref. [17]:

$$\eta(n\bar{n}) = 0.90 \quad (2.8)$$

Here it is worth to notice that the Coulomb corrections  $E_C(nL)$  to the light meson masses are small,  $|E_C| \leq 100$  MeV and can be neglected in the first approximation. The results of the exact calculations for a linear plus Coulomb potential Eq. (2.3) will be presented in Section IV and in the Appendix.

The self-energy term enters the squared mass  $\bar{M}^2$  in such a way that it gives rise to an important negative constant  $C_0$ ,

$$C_0 = -\frac{32\eta\sigma_0}{\pi} \quad (2.9)$$

so that the mass formula for the squared meson mass is

$$\bar{M}^2(nL) = M_0^2 - \frac{4\sigma_0 \langle r^{-1} \rangle L(L+1)}{M_0} - \frac{32\eta\sigma_0}{\pi} + \frac{256\sigma_0^2\eta^2}{\pi^2 M_0^2}, \quad (2.10)$$

i.e. it is proportional to  $\sigma$  and does not contain any free parameter. In Eq. (2.10) the contributions of the small terms  $\Delta_{\text{str}}^2$  and  $2\Delta_{\text{str}}\Delta_{\text{SE}}$  were neglected to show the most important features of the meson spectra. On the contrary the term  $\Delta_{\text{SE}}^2 \geq 0.10$  GeV<sup>2</sup> is not small for any state and therefore is kept in the mass formula (2.10).

An important next step refers to the approximation for the eigenvalues  $M_0^2(nL)$  of the SSE valid for the linear potential  $\sigma_0 r$  :

$$M_0^2(\text{approx}) = [8L + 4\pi\xi(nL)n_r + 3\pi]\sigma_0. \quad (2.11)$$

This formula with  $\xi = 1.0$  reproduces the exact values of  $M_0^2(nL)$  with an accuracy better than 2% for all  $nL$ -states with the exception of the  $1S$  and  $1P$  states where the accuracy is 3-6% [7]. In Eq. (2.11) the coefficient  $\xi(nL) \simeq 1.0$  weakly depends on  $L$  and slightly decreases with growing  $n_r$ , e.g. for the  $4S$  state  $\xi(4S) = 0.99$  while  $\xi(4F) = 0.96$ . In what follows in most cases we put  $\xi(nL) = 1.0$ .

Then with the use of the expression (2.11) and redefining the matrix element  $\langle r^{-1} \rangle = \sqrt{\sigma_0} \langle \rho^{-1} \rangle$  where  $\langle \rho^{-1} \rangle$  is already independent of  $\sigma_0$ , one can rewrite the mass formula Eq. (2.10) in the following way,

$$\bar{M}^2(nL) = (\alpha'_L)^{-1} L + [4\pi n_r + b(nL)]\sigma_0 \quad (2.12)$$

giving for the  $L$ -trajectory,

$$L = \alpha'_L \bar{M}^2(nL) + \alpha_L(n), \quad (2.13)$$

the Regge slope (in general  $n_r \neq 0$ ):

$$(\alpha'_L)^{-1} = \sigma_0 [8 - \delta(nL)] \equiv \sigma_0 \left[ 8 - \frac{\sqrt{2} \langle \rho^{-1} \rangle (L+1)}{\sqrt{L + \frac{\pi n_r}{2} + \frac{3\pi}{8}}} \right]. \quad (2.14)$$

For the leading  $L$ -trajectory ( $\langle \rho^{-1} \rangle \sqrt{L+1} \sim \text{constant}$ ) the slope is given by the constant [7]

$$(\alpha'_L)^{-1} = (6.95 \pm 0.02)\sigma_0$$

or

$$\alpha'_L = \frac{1}{6.95\sigma_0} = 0.80 \text{ GeV}^{-2} \quad \text{for } \sigma_0 = 0.18 \text{ GeV}^2, \quad (2.15)$$

which is in good agreement with the experimental value  $\alpha'_L(\text{exp}) = 0.81 \pm 0.02 \text{ GeV}^{-2}$ . For the orbital excitations with a fixed  $n_r > 0$ ,  $\alpha'_L(n_r)$  appears to be a bit smaller since for them  $\delta(nL)$  in Eq. (2.14) is smaller, e.g.  $\delta(n_r = 1) = 0.85 \pm 0.05$  and  $\delta(n_r = 3) \simeq 0.50$  while  $\delta(n_r = 0) = 1.05$ . Then for  $\sigma_0 = 0.18 \text{ GeV}^2$

$$\begin{aligned} \alpha'_L(n_r = 1) &= 1/[7.2\sigma_0] = 0.77 \text{ GeV}^{-2}, \\ \alpha'_L(n_r = 3) &= 1/[7.5\sigma_0] = 0.74 \text{ GeV}^{-2} \end{aligned} \quad (2.16)$$

However, this slope gives larger values for the radial excitations, e.g.  $\bar{M}(2P) = 1.82 \pm 0.03 \text{ GeV}$  while the expected experimental number is  $\bar{M}(2P) \leq 1.70 - 1.75 \text{ GeV}$  [2], [3].

From Eq. (2.10) it follows that the constant  $b(nL)$  in Eq. (2.12) is

$$b(nL) = 3\pi - \frac{32\eta}{\pi} + \frac{32\eta^2}{\pi^2(L + \frac{\pi n_r}{2} + \frac{3\pi}{8})}. \quad (2.17)$$

As was stressed in Ref. [7], for the  $b(1S)$  meson it is more precise to use the exact eigenvalue with  $M_0^2(1S) = 9.967\sigma_0$  instead of the approximation (2.11) so that for the leading  $L$ -trajectory ( $\eta = 0.90$ ) one finds

$$\begin{aligned} b(1S) &= 3\pi - \frac{32\eta}{\pi} + \frac{256\eta^2\sigma_0}{\pi^2 M_0^2}, \\ &= 0.257 + \frac{256\eta^2}{9.967\pi^2} = 2.365. \end{aligned} \quad (2.18)$$



Then from the mass formula (2.12) the intercept of the leading  $L$ -trajectory,

$$\alpha_L(\bar{M}^2 = 0) = -\alpha'_L b(1S) \sigma_0 = -2.365/6.95 = -0.34, \quad (2.19)$$

does not depend on the string tension and is a universal number. With 10% accuracy it coincides with the experimental number  $\alpha_L(0)_{\text{exp}} = 0.30 \pm 0.02$  [7].

For  $n_r \neq 0$  the intercept of the  $L$ -trajectory is

$$\begin{aligned} \alpha_L(n_r, \bar{M}^2 = 0) &= -\alpha'_L(n_r)[4\pi n_r + b(nL)]\sigma_0 \\ &= -\frac{0.257 + \frac{2.626}{L+\pi n_r/2+3\pi/8} + 4\pi n_r}{8 - \delta(nL)} \quad (n_r \neq 0). \end{aligned} \quad (2.20)$$

In the intercept (2.20) the term  $b(nL)$  is small as compared to  $4\pi n$  (the largest correction is for the  $S$ -wave states but even then it is  $\leq 10\%$ ) and can be neglected in first approximation. Then also neglecting  $\delta(nL)$  compared to 8 one obtains

$$\alpha_L(n_r) \simeq -\frac{\pi n_r}{2}, \quad (2.21)$$

which does not depend on  $L$  and  $\sigma_0$ . For the neighbouring intercepts the difference is equal to the following constant,

$$\alpha_L(n_r + 1) - \alpha_L(n_r) = -\pi/2 = -1.57. \quad (2.22)$$

The magnitude of the intercept is rather large due to the presence of the large number  $4\pi n_r \sigma_0$  in the eigenvalue  $M_0^2(nL)$  (or  $\bar{M}^2$  (2.12)). Note that another large number,  $3\pi\sigma_0$ , which is present in  $M_0^2(nL)$ , is practically cancelled by the constant  $C_0$ , Eq. (2.9), coming from the self-energy contribution. Now one can present the masses of the radials in the form of the  $n_r$ -trajectory Eq. (1.1):

$$\bar{M}^2(n_r, L) = M^2(0, L) + \Omega_0 n_r \quad (L \text{ fixed}), \quad (2.23)$$

where from the mass formula (2.10) one finds for the linear potential the following expression for  $\Omega_0$

$$\Omega_0 = [4\pi\sigma_0\xi(nL)][1 - \chi(nL)] \simeq 1.90 - 2.10 \text{ GeV}^2 \quad \text{for } \sigma_0 = 0.18 \text{ GeV}^2. \quad (2.24)$$

$$(\chi(nL) = (b(nL) - b(n+1L))/4\pi)$$

In Eq. (2.24)  $0.95 \leq \xi(nL) \leq 1.05$  and  $0.05 \leq \chi \leq 0.10$  for all  $nL$  states ( $n_r \leq 4, L \leq 4$ ) so that  $\Omega_0$  is only 5%-10% smaller than  $4\pi\sigma_0$ .

Thus for the linear potential we have obtained

- (i) The masses of the radials lie on linear  $n_r$ -trajectories as in Eq. (1.1);
- (ii) The slope  $\Omega_0$  does not depend on  $L$  (with 95% accuracy) in agreement with experimental observations;
- (iii) However, numerically the value of  $\Omega_0$  turns out to be  $\simeq 1.6$  times larger than the value extracted from the experimental data [3].

To explain this phenomenon we suggest below a physical mechanism which can be applied to highly excited mesons.

### III. MESON MASSES AND QUARK PAIR CREATION

The effective Hamiltonian derived from the QCD Lagrangian with the use of the Fock-Feynman-Schwinger representation[18] is based on the quenched approximation, where the quark determinant is replaced by unity. Based on the width-to-mass ratio and on the existence of linear Regge trajectories for the mesons it is usually argued that the effects of the sea quark loops coming from the quark determinant cannot be large and are estimated to be around 10%. The same estimate of this correction is obtained from lattice calculations for the unquenched low-lying hadrons[19]. Moreover, lattice calculations of the  $Q\bar{Q}$  static potential up to 1.0 – 1.5 fm do not show a significant difference between quenched and unquenched calculations [13]-[20].

It can be shown that the radial excitations and high orbital excitations ( $L \geq 4$ ) have sizes exceeding 1.5 fm (see Table I) and therefore one should reconsider possible effects of quark loops on the large-size mesons. A dedicated study on the lattice [14] shows a flattening of the static potential or decreasing of the string tension at separations  $r > 1$  fm. However, at present lattice points have large errors at such distances, quickly deteriorating with increasing  $r$  and one cannot extract the exact form of the static potential at large  $r$  from lattice data.

Above the threshold of  $q\bar{q}$  pair creation the static  $Q\bar{Q}$  pair could decay into two heavy-light mesons with mass  $M_{\text{HL}} = 2m_Q + 2E_{\text{HL}}$  where  $E_{\text{HL}}$  is the excitation energy of the heavy-light meson which can be calculated in the framework of the formalism presented in Ref. [21] and is found to be  $E_{\text{HL}}(\alpha_s = 0) = 0.73$  GeV and  $E_{\text{HL}}(\alpha_s = 0.39) = 0.53$  GeV for a  $b$ -quark mass  $m_b = 4.8$  GeV.

For the  $c$  quark with  $m_c = 1.4$  GeV the values are close:  $E_{\text{HL}}(\alpha_s = 0) = 0.76$  GeV and  $E_{\text{HL}}(\alpha_s = 0.39) = 0.58$  GeV are obtained[22]. So one can expect that for lighter quarks  $E_{\text{LL}}$  is also  $\simeq 0.7 - 0.6$  GeV and the threshold of  $q\bar{q}$  pair creation inside the world-sheet of the string to be  $M_{\text{thr}} = 1.2 - 1.4$  GeV in accord with the experimental  $\rho - \rho$  threshold Eq. (1.2). Expressing this value in terms of the distance  $R_1$ :  $M_{\text{thr}} = \sigma_0 R_1$  one finds the number

$$R_1 = 1.3 - 1.5 \text{ fm}$$

close to the value  $R_1$  in Eq. (1.3).

At this point one should stress that the phenomenon discussed, viz the pair creation just on the string, does not necessarily exhausts all possible meson decay mechanisms or the true hadronization of the mesons. Namely, as was shown in Ref. [12], pions are directly coupled to the quark (antiquark) at the ends of the string and can be emitted from there without breaking it.

Indeed, bosonization of quark degrees of freedom in Ref. [12] leads to the following term in the Lagrangian in the local limit:

$$\Delta\mathcal{L}^{(1)} = \int dt d^3x \left[ \bar{q}(x) \sigma|\vec{x}| \gamma_5 \frac{\pi^a \lambda^a}{F_\pi} q(x) \right], \quad (3.1)$$

where the string starts from the antiquark position  $\vec{x} = 0$ ; the field  $\pi^a$  is the octet of Nambu-Goldstone mesons, and  $F_\pi = 93$  MeV.

The same operator  $\Delta\mathcal{L}^{(1)}$  between quark bound states can be rewritten with the use of the Dirac equation as follows

$$\Delta\mathcal{L}^{(1)} = g_A^q \text{Tr} \bar{q} \gamma^\mu \gamma_5 \omega_\mu q, \quad (3.2)$$

with

$$\omega_\mu = \frac{i}{2F_\pi} (u \partial_\mu u^\dagger - u^\dagger \partial_\mu u) u = \exp \left( i \gamma_5 \frac{\pi^a \lambda^a}{2F_\pi} \right), \quad g_A^q = 1.0. \quad (3.3)$$

From this expression one can see that  $\Delta\mathcal{L}^{(1)}$  describes the emission of an arbitrary number of Nambu-Goldstone mesons from the quark position and therefore may describe pionic and double pionic hadron decays while the string plays the role of a spectator and stays intact.

At the same time  $q\bar{q}$  pairs around the string (sea quarks) should be identified with the loops of the determinant which can be written as [22, 23]:

$$\ln \det(m^2 + D^2) = \int d^4x \int_0^\infty \frac{ds}{s} \exp(-m^2 s) (Dz)_{xx} \exp \left( - \int_0^s \frac{\dot{z}^2 d\tau}{4} \right) W(C). \quad (3.4)$$

The integral  $(Dz)_{xx}$  in Eq. (3.4) is taken along the closed loop  $C$  from some point  $x$  back to  $x$  and contains an integral over loops of all sizes. Alternatively, one can separate the quark determinant into parts of small and large eigenvalues as in Ref. [14],

$$\det(A) = \det_{\text{IR}}(A) \det_{\text{UV}}(A), \quad (3.5)$$

where  $\det_{\text{IR}}$  takes into account the small eigenvalues (large loops)  $\lambda_n \leq \Lambda_{\text{cut}}$  while  $\det_{\text{UV}}$  contains the large eigenvalues. The latter correspond to the contribution of small virtual loops which should be properly renormalized.

In the physical picture  $\det_{\text{IR}}$  corresponds to the chiral effects which disappear in  $\det(m^2 + D^2)$  for large  $m_q$ :  $m_q^2 \gg \Lambda_{\text{QCD}}^2$  together with effects of large loops.

At this point it is important to stress that treating the resonances as quasistationary states one should always consider Green's functions and correspondingly Wilson  $q\bar{q}$  loops of finite time extension  $T$ ,  $T \sim 1/\Gamma(nL) \sim 1 - 2$  fm.

For such finite times one can write a general expansion for the original Wilson loop of the  $q\bar{q}$  meson with pair creation due to the quark determinant Eq. (3.4) as follows

$$\langle W(C) \det(m + D) \rangle = W_0(C) + \frac{a_1}{N_c} W_1(C, C_1) + \frac{a_2}{N_c^2} W_2(C, C_1, C_2) + \dots, \quad (3.6)$$

where the coefficients  $a_i = O(1)$  and higher Wilson loops  $W_i, i \geq 1$ , are averaged products of the  $i + 1$  Wilson loops, i.e.

$$W_1(C, C_1) = \langle \langle W(C) W(C_1) \rangle \rangle, \quad W(C) = \frac{1}{N_c} \text{Tr} \hat{W}(C). \quad (3.7)$$

It is clear that when  $T \rightarrow \infty$  and  $r \geq R_1$  (so that decay is energetically possible) the asymptotics of the r.h.s. of Eq. (3.6) is

$$\exp(-\sigma r T) + \frac{a_1}{N_c} \exp(-T(M_1 + M_2)) + \frac{a_2}{N_c^2} \exp(-T \sum M_i) + \dots, \quad (3.8)$$

where  $\sum M_i$  is the sum of the masses of the decay products ( $i = 1, 2$  in the simplest case and  $i = 1 \dots k$  for meson decay into  $k$ -particles etc.). So, if  $T \rightarrow \infty$  the resonances are dying out and the second term in Eq. (3.8) is dominant, which means that only the products of meson decay are left.

However, for finite  $T \simeq 1 - 2$  fm the situation is different and one can expect a delicate balance between the large  $N_c$  limit (suppressing  $q\bar{q}$  pair creation) and large times  $T$  (preferring large internal loops). This statement is the dynamical basis of our main assumption

about the existence of a specific state of the string with effectively a hole inside the world sheet which obeys the area law with a reduced (renormalized) string tension  $\sigma^* = \sigma(r)$ .

Thus we introduce the new concept of a transitional regime which in terms of  $Q\bar{Q}$  separations  $r$  refers to the region

$$R_1 \leq r \leq R_2$$

where  $R_1 \sim 1.2 - 1.4$  fm.  $R_2 \sim 2.5$  fm corresponds to high excitations with energies  $E^* \sim 2.5$  GeV.

In this region, due to relatively small quark loops and correspondingly small holes in the string world sheet, the string tension is nonperturbatively renormalized and decreases with growing  $r$ . While the loops are still virtual, their presence does not lead to actual string breaking (with appreciable probability) even though the energy of the string for  $r \geq R_1$  is sufficient for meson decay. We suggest here that only for much larger distances,  $r \geq R_2 \simeq 2.5$  fm the string breaking happens with large probability.

A first argument in favour of this picture is that highly excited mesons of large radii do exist and lie on the corresponding linear Regge trajectories, while their characteristics can be computed as in the QCD string approach, neglecting decay channels. At the same time at such large distances the string tension cannot remain intact and should be strongly decreased by the appearance of holes inside the string world sheet due to pair creation.

The second argument refers to the experimental information about strong decay modes. The first strong decays without Goldstone particles is observed only for  $f_0(1370) \rightarrow \rho - \rho$  and  $f_2(1565) \rightarrow \rho_0 - \rho_0$  decays in accord with our picture that  $\sigma = \text{constant}$  at distances  $r \leq R_1$  or excitations  $E^* \leq 1.4$  GeV.

For higher excitations, in the range  $1.4 \text{ GeV} \leq E^* \leq 2.5 \text{ GeV}$ , at present only several strong decays like  $f_2(1640) \rightarrow \omega - \omega$ , (seen);  $\pi_2(1670) \rightarrow \omega - \rho$  (branching  $\sim 2.7\%$ ), and  $f_4(2050) \rightarrow \omega - \omega$  (branching  $\sim 25\%$ ) have been measured and in all these cases the branching ratios of decays without Goldstone particles are never large.

The third argument refers to the r.m.s. radii  $R(nL) = \sqrt{\langle r^2 \rangle_{nL}}$  of the radials which are ( $n_r \neq 0$ ) calculated for the linear potential with  $\sigma_0 = 0.19 \text{ GeV}^2$  (see Table I). (It is worth to notice that the numbers given for  $R(nL)$  represent the lower limits of the true r.m.s. radii, since they correspond to larger meson masses and the actual values of  $R(nL)$  are about 20-50% larger (see Table VI). From the values of  $R(nL)$  given here one can see that among the ground states only the  $1G$  state has  $R(1G) \simeq 1.4$  fm, while for the  $2L$  and

TABLE I: The light meson r.m.s. radii  $R(nL)$  in fm for the  $\sigma_0 r$  potential with  $\sigma_0 = 0.19 \text{ GeV}^2$ .

$n_r \setminus L$	0	1	2	3	4
0	0.80	1.02	1.21	1.37	<u>1.51</u>
1	1.22	<u>1.31</u>	<u>1.52</u>	<u>1.70</u>	<u>1.77</u>
2	<u>1.53</u>	<u>1.66</u>	<u>1.78</u>	<u>1.90</u>	<u>2.00</u>

the  $3L$  states (with the exception of the  $2S$  state with relatively small r.m.s. radius equal to 1.21 fm)  $R(nL)$  are in the range:

$$\begin{aligned}
 1.4 \text{ fm} < R(2L) < 1.8 \text{ fm} \quad (n_r = 1), \\
 1.7 \text{ fm} < R(3L) < 2.0 \text{ fm} \quad (n_r = 2).
 \end{aligned}
 \tag{3.9}$$

The values of  $M(\text{exp})$  for all states underlined in Table I are shifted down compared to the theoretical values calculated with the same linear potential that gives a good description of the orbital excitations with  $n_r = 0$ . This example agrees with our estimate of the characteristic size  $R_1 = 1.4 \text{ fm}$  where the pair creation is beginning to affect the string tension  $\sigma(r)$ .

The r.m.s. radii in Table I also show that even for the linear potential  $R(nL) \geq 1.90 \text{ fm}$  for such states as the  $3F$  states:  $f_4(2290)$ ,  $f_3(2280)$ ,  $a_4(2280)$ , and  $a_3(2310)$ [2].

At this point it is important to stress the difference and similarity of our approach with that in Refs. [9], [10]. In both approaches it is stressed that the  $q\bar{q}$  pair creation is responsible for the renormalization of the string tension and therefore the unquenched string tension is lower than in the quenched case. Moreover in Ref. [10] as well as in the present paper it is emphasized that even when level crossing occurs, i.e. when  $V(r)$  equals  $2M_{\text{HL}}$ , the string potential can be used throughout, only the string tension being renormalized.

The difference between both approaches is in the meaning of this renormalization. We assume here that there exists a universal (quantum number independent) prehadronization stage when small quark loops attenuate the string tension, while one can still neglect the influence of specific decay channels which produce the hadronic shift.

It was already realized in Refs. [9, 10] that the very fact of the occurrence of smooth Regge trajectories and ordered hadronic spectra is difficult to explain if the hadronic shifts are essentially important, since the latter depend on the concrete hadronic channels involved and vary irregularly from channel to channel.

In the suggested picture due to the universal predecay (prehadronization) stage with renormalized (attenuated) string tension not only can the spectrum be calculated, but the notion of linear Regge trajectories, both radial and orbital, is kept intact.

#### IV. MODIFIED CONFINING POTENTIAL

From the physical picture discussed in Section III and the introduction it follows that up to the characteristic distance  $R_1 \sim 1.2 - 1.4$  fm the string tension  $\sigma$  is constant, while for larger  $r$  it depends on the  $q\bar{q}$  separation as in Eq. (1.6). We propose here the nonperturbative potential  $\sigma(r)r$  with the string tension taken in the following form:

$$V_{\text{NP}}(r) = \sigma(r)r, \quad \sigma(r) = \sigma_0 \left[ 1 - \gamma \frac{\exp(\sqrt{\sigma_0}(r - R_1))}{B + \exp(\sqrt{\sigma_0}(r - R_1))} \right]. \quad (4.1)$$

In the definition Eq. (4.1) the constant  $\gamma$  determines the value of the string tension at large separations so that

$$\sigma_2 = \sigma(r \geq 2.5 \text{ fm}) \simeq \sigma_0(1 - \gamma). \quad (4.2)$$

Note that  $\sigma_0 \sim 0.18 - 0.19 \text{ GeV}^2$  defines the common scale of the modified string potential and can be fixed by the Regge slope of the leading  $L$ -trajectory.

In general our calculations are performed with the potential  $V(r)$  Eq. (2.3) containing the perturbative potential  $V_{\text{P}}(r)$ ,

$$V_{\text{P}}(r) = -\frac{4\alpha_s}{3r}, \quad (4.3)$$

where for the strong coupling constant the value  $\alpha_s = 0.30$  is taken.

The best description of the meson spectra was obtained for the following set of the parameters in  $\sigma(r)$ :

$$\gamma = 0.40, \quad R_1 = 6 \text{ GeV}^{-1}, \quad B = 20.0, \quad (4.4)$$

while the values of  $\sigma_0 = 0.185 \pm 0.005 \text{ GeV}^2$  and  $\alpha_s = 0.30 \pm 0.08$  can vary in narrow ranges. In Fig. 1 this potential is drawn for the parameters Eq. (4.4),  $\alpha_s = 0$  and  $\sigma_0 = 0.19 \text{ GeV}^2$ .

At the distance  $R_2(nL) = 2.5$  fm the value  $\sigma_2 = 0.116 \text{ GeV}^2$  turns out to be rather small, a value 40% smaller than  $\sigma_0 = 0.19 \text{ GeV}^2$ .

The spin-averaged meson masses  $\bar{M}(nL)$  are calculated solving the SSE Eq. (2.2) with the modified potential  $V(r)$ . Their values will be given in the next section. Here only some characteristic features of the SSE solutions for the modified potential will be discussed.

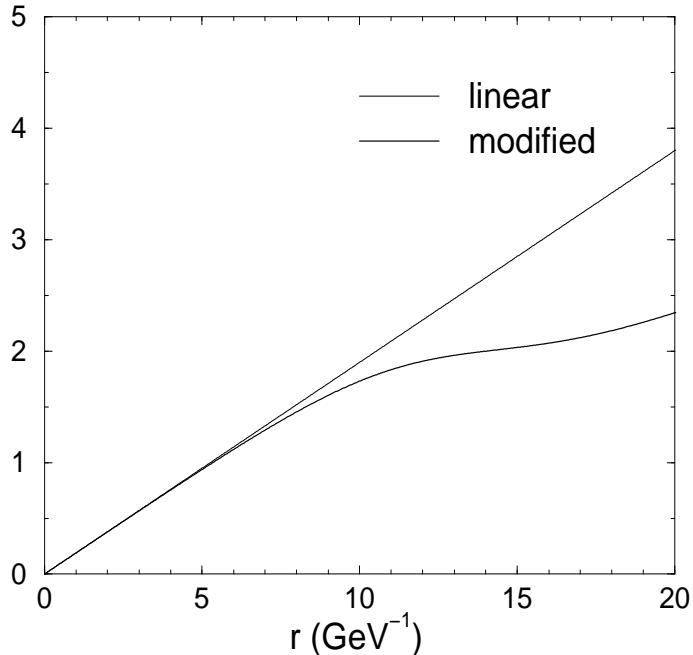


FIG. 1: Modified potential with parameters given in Eq. (4.4). For reference a simple linear potential with  $\sigma = 0.19$  is also plotted.

TABLE II: The values of  $\bar{\sigma}(nL)$  (in  $\text{GeV}^2$ ) for the potential  $V(r)$  Eq. (4.1) with the parameters Eq. (4.4) ( $\sigma_0 = 0.19 \text{ GeV}^2$ ,  $\alpha_s = 0.30$ ).

$n_r \setminus L$	0	1	2	3	4
0	0.188	0.187	0.184	0.179	0.168
1	0.183	0.176	0.164	0.153	0.150
2	0.165	0.155	0.154	0.154	0.150
3	0.156	0.156	0.154	0.154	0.150

First, the average values of the string tension  $\bar{\sigma} = \langle \sigma(r) \rangle_{nL}$  turns out to be almost constant for the ground states ( $n_r = 0$ ,  $L \leq 3$ ), while for the radials with  $n_r \geq 2$   $\bar{\sigma}$  is already 20% smaller, see Table II.

Secondly, the kinetic energy and therefore the constituent quark mass  $\mu(nL)$  does practically not change for the ground states in contrast to the high excitations where the string size is growing and the quark kinetic energy is becoming significantly smaller. In Table III  $\mu(nP)$  for the  $nP$  states for the potential Eq. (4.1) with  $\alpha_s = 0$  and the linear potential  $\sigma_0 r$  are compared (in both cases  $\sigma_0 = 0.182 \text{ GeV}^2$ ).



TABLE III: The constituent masses  $\mu(nP)$  for the modified potential Eq. (4.1) with  $\alpha_s = 0$  and  $\mu_0(nP)$  for the potential  $\sigma_0 r$  with  $\sigma_0 = 0.182 \text{ GeV}^2$  in both cases.

$n_r$	0	1	2	3	4
$\mu(nP)$	0.424	0.430	0.441	0.559	0.616
$\mu_0(nP)$	0.451	0.582	0.697	0.787	0.872

TABLE IV: The spin-averaged meson masses of the  $nS$  states (in GeV) for the modified potential  $V(r)$  Eq. (4.1) with the parameters Eq. (4.4),  $\alpha_s = 0.30$  and  $\sigma_0 = 0.19 \text{ GeV}^2$  \*.

$nS$	1S	2S	3S	4S	5S
$\bar{M}(nS)$	0.618	1.400	1.868	2.176	2.502
	(0.673)	(1.520)	(2.122)	(2.602)	(3.006)
$\bar{M}(nS)_{\text{exp}}$	0.612	$1.41 \pm 0.02$	$\pi(1.80)$	$\rho(2.15)$	

\* The numbers in brackets correspond to the Cornell potential Eq. (5.1) with the same  $\alpha_s = 0.30$  and  $\sigma_0 = 0.19 \text{ GeV}^2$ .

From Table III one can see that for the  $4P(5P)$  states the difference between the constituent masses is large and reaches  $\sim 30\%$ . Note that for the modified potential the relations (2.5) are not valid anymore and

$$\langle \sigma(r)r \rangle_{nL} > 2\mu(nL) \quad (4.5)$$

and therefore in this case the string correction  $\Delta_{\text{str}}$  is given by a more general expression than in Eq. (2.4) [7]:

$$\Delta_{\text{st}} = -\frac{\bar{\sigma} \langle r^{-1} \rangle L(L+1)}{\mu(6\mu + \langle \sigma(r)r \rangle)}. \quad (4.6)$$

Also in the self-energy term  $\Delta_{\text{SE}}(nL)$  Eq. (2.7),  $\bar{\sigma}$  must be used instead of  $\sigma_0$ .

## V. THE MASSES OF THE RADIALS

The masses of the radial excitations for the modified potential Eq. (4.1) with the Coulomb interaction included are presented in Tables IV-VI for the parameters given in Eq. (4.4),  $\alpha_s = 0.30$ , and the string tension  $\sigma_0 = 0.19 \text{ GeV}^2$ . In all cases the calculated meson masses turn out to be in good agreement with the existing experimental data.

TABLE V: The spin-averaged meson masses of the  $nP$ -states (in GeV) for the potential  $V(r)$  Eq. (4.2) with the parameters Eq. (4.4),  $\alpha_s = 0.30$  and  $\sigma_0 = 0.19 \text{ GeV}^2$  \*.

$nP$	$1P$	$2P$	$3P$	$4P$
$\bar{M}(nP)$	1.190 (1.263)	1.715 (1.933)	2.090 (2.438)	2.388 (2.859)
$\bar{M}(nP)_{\text{exp}}$	1.252 for $\bar{M}(a_J(1P))$	$a_1(1.70)$ $a_2(1.75)$	$a_1(2.10)$ $a_0(2.05)$	$a_1(2.34)$ $f_0(2.34)$
	1.245 for $\bar{M}(f_J(1P))$	$f_2(1.65)$	$f_0(2.095)$	

\*) see footnote to Table IV.

The numbers in brackets in Table IV are the masses calculated for the Cornell potential,

$$V_C(r) = -\frac{4\alpha_s}{3r} + \sigma_0 r. \quad (5.1)$$

From a comparison of the numbers given one can see that with the modified nonperturbative potential the mass of the  $4S(5S)$  states appears to be 400 MeV (500 MeV) lower than for the Cornell potential Eq. (5.1), while for the  $1S$  and  $1P$  states the difference is only about 60 MeV.

We observe the same picture for the  $P$ -wave and higher excitations when already for the  $2P$  ( $3P$ ) states the spin-averaged mass is  $\simeq 200 \text{ MeV}$  ( $350 \text{ MeV}$ ) smaller due to the modification of the string potential (see Table V, where the numbers in the parentheses are calculated with the Cornell potential Eq. (5.1) with the same  $\alpha_s$  and  $\sigma_0$ ).

The calculated masses of the  $nS$  and  $nP$  states as well as the  $nD$  and  $nF$  states (see Table VI) appear to be in good agreement with experiment. However, for the  $nD$  and  $nF$  states a better agreement is obtained for smaller values of the strong coupling constant and the numbers given in Table VI refer to  $\alpha_s = 0.21$ . This fact may be connected with a suppression of one-gluon-exchange for large-size mesons.

Thus one can conclude that due to the attenuation of the string tension in the potential Eq. (4.1) the masses of the radials turn out to be  $\simeq 100 - 200 \text{ MeV}$  (for the  $2L$  states),  $\simeq 300 \text{ MeV}$  (for the  $3L$  states), and  $\simeq 350 - 400 \text{ MeV}$  smaller than for the standard linear potential. It is of interest also to compare the r.m.s. radii  $R(nL)$  of the radials for the modified potential (see Table VII) with that for the  $\sigma_0 r$  potential given in Table I.

From this comparison one can find out that the size of the  $2P$  mesons is changing from

TABLE VI: The spin-averaged meson masses (in GeV) for the  $nD$  and  $nF$  states for the potential  $V(r)$  Eq. (4.2) with the parameters Eq. (4.4),  $\alpha_s = 0.21$ , and  $\sigma_0 = 0.19 \text{ GeV}^2$ .

$n$	$1D$	$2D$	$3D$	$1F$	$2F$	$3F$
$\bar{M}(nD)$	1.628	1.973	2.290	1.926	2.214	2.480
$M(\text{exp})$	$\rho_3(1.67)$	$\pi_2(2.0)$	$\pi(2.25)$	$a_4(2.01)$	$a_4(2.26)$	-
	$\rho_3(1.69)$	$\rho_3(1.98)$	$\rho_3(2.30)$	$a_3(2.03)$	$a_3(2.28)$	

TABLE VII: The r.m.s. radii  $R(nL)$  (in fm) of the  $nL$  states for the potential  $V(r)$  (41) with the parameters (43),  $\alpha_s = 0.30$ , and  $\sigma_0 = 0.19 \text{ GeV}^2$ .

state \ $L$	0	1	2	3	4
$1L$	0.74	1.03	1.29	1.61	2.10
$2L$	1.32	1.74	2.22	2.61	2.74
$3L$	2.22	2.53	2.63	2.67	2.81
$4L$	2.58	2.66	2.81	2.97	3.09

$R(2P) = 1.31 \text{ fm}$  to  $1.74 \text{ fm}$  while the mass  $\bar{M}(2P)$  is shifted down by about  $200 \text{ MeV}$ . From Table VII it is also seen that for the modified potential highly excited radials, like the  $3P$  mesons, have very large r.m.s. radii  $\simeq 2.5 - 2.8 \text{ fm}$ , in particular the experimentally observed mesons  $\rho(4S)$  and  $a_J(3P)$  have  $R(nL) \sim 2.5 - 2.6 \text{ fm}$ .

## VI. THE SLOPE OF THE $n_r$ -TRAJECTORIES

There are not many radial excitations with well established masses which are included in the PDG compilation [1]. Most radials were observed in the BNL and Crystal Barrel experiments and discussed in many papers for the last five years (see Ref. [2]-[4] and references therein). Here we present the values of the slope  $\Omega$  defining the  $n_r$ -trajectory Eq. (1.1).

Since we have calculated here only the spin-averaged masses of the radials, correspondingly just for them the  $n_r$ -trajectory Eq. (1.1) will be calculated below. Although in many cases there exists a large uncertainty in the values of  $\bar{M}(nL)$  we give below in Table VIII several well established masses taking into account that the spin splittings are small.

Then taking the difference between the neighbouring  $\bar{M}^2$  values one can calculate the

TABLE VIII: The experimental spin-averaged masses of the radials

$L$	$1S$	$2S$	$1P$	$2P$	$3P$	$4P$
$\bar{M}(nL)$	0.612	$1.42 \pm 0.04$	$1.25 \pm 0.05$	$1.70 \pm 0.05$	$2.07 \pm 0.03$	$\sim 2.34$
$L$	$1D$	$2D$	$3D$	$1F$	$2F$	
$\bar{M}(nL)$	$1.67 \pm 0.02$	$2.00 \pm 0.02$	$\simeq 2.30$	$2.02 \pm 0.01$	$2.30 \pm 0.01$	

values of  $\Omega$  in Eq. (1.1):

$$\begin{aligned}
 \Omega_{\text{exp}}(S) &= 1.64 \pm 0.11 \text{ GeV}^2, \\
 \Omega_{\text{exp}}(P) &= 1.35 \pm 0.25 \text{ GeV}^2, \\
 \Omega_{\text{exp}}(D) &= 1.21 \pm 0.16 \text{ GeV}^2, \\
 \Omega_{\text{exp}}(F) &= 1.21 \pm 0.08 \text{ GeV}^2,
 \end{aligned} \tag{6.1}$$

which in some cases have a rather large experimental error, but for  $L \neq 0$  practically coincide with the value  $\Omega = 1.15 - 1.30 \text{ GeV}^2$  obtained in Ref. [3]. Unfortunately, among the  $nS$  states the very important ones  $\rho(3S)$  and  $\pi(4S)$  are still not observed and the known value of  $\Omega_{\text{exp}}(nS)$  obtained from the difference of  $\bar{M}^2(2S)$  and  $\bar{M}^2(1S)$  appears to be 20% larger than in Ref. [3] and close to our number Eq. (6.3).

From the meson masses given in Tables IV-VI one can calculate now the theoretical values of the slope  $\Omega_{\text{thr}}$  taking for the mass  $\bar{M}^2(1L)$  with  $n_r = 0$  in Eq. (1.1) the experimental number. Then one finds

$$\begin{aligned}
 \Omega_{\text{th}}(P) &= 1.38 \pm 0.05 \text{ GeV}^2, \\
 \Omega_{\text{th}}(D) &= 1.29 \pm 0.06 \text{ GeV}^2, \\
 \Omega_{\text{th}}(F) &= 1.22 \pm 0.13 \text{ GeV}^2.
 \end{aligned} \tag{6.2}$$

However, for the  $nS$  radials the slope was found to be slightly dependent on  $n_r$ .

$$\Omega_{\text{th}}(S) = 1.60 - 1.45 \text{ for } n_r = 0, 1, 2, \tag{6.3}$$

which is close to the experimental value  $\Omega_{\text{exp}} = 1.6 \pm 0.1 \text{ GeV}^2$  obtained for the first excited state, while for higher  $S$ -excitations  $\Omega_{\text{th}}$  was found to be  $\sim 15\%$  smaller and equal to

$$\bar{M}^2(4S) - \bar{M}^2(3S) = 2.18^2 - 1.87^2 = 1.26 \text{ GeV}^2, \tag{6.4}$$

We can conclude that in the physical picture where the confining potential is modified due to  $q\bar{q}$  pair creation, the slope  $\Omega$  is decreasing from a value  $\sim 2.0 \text{ GeV}^2$  for the standard linear potential to values in the range  $1.2 - 1.35 \text{ GeV}^2$  for mesons with  $L \neq 0$ .

## VII. CONCLUSIONS

We have considered here the light meson orbital and radial excitations using the effective Hamiltonian derived from QCD under definite and verifiable assumptions. In the QCD string approach the spin-averaged meson mass  $\bar{M}(nL)$  can be calculated through the only scale parameter - the string tension and does not contain any arbitrary subtraction constants, since nonperturbative quark mass renormalization is taken into account as in Ref. [12]. The suggested formalism allows to resolve three old painstaking problems:

To determine the origin of the constituent mass for a light quark which is derived to be the average of the quark kinetic energy operator and can be computed through the string tension;

To obtain the correct slope of the Regge trajectory when the string moment of inertia is taken in account;

To obtain the correct absolute values of the light meson masses and as a consequence the correct value of the  $L$ -trajectory intercept (which refers to the spin averaged meson masses). The use of the  $L$ -trajectories is very convenient since they are universal, i.e. in the closed-channel approximation they are the same for isovector and isoscalar mesons.

In Ref. [7] this formalism was successfully applied to the orbital excitations with  $n_r = 0$  when for the linear confining potential the string tension was taken constant. However, in an attempt to describe the radial excitations one encounters a serious problem - the Regge slope of the  $n_r$ -trajectories calculated with the same potential appears to be 1.5-1.7 times larger than in experiment.

This phenomenon, the lowering of the masses of the highly excited mesons, is connected in our picture with large sizes of the high excitations, which can be as large as 2.5 fm and lead to the formulation of the concept of the predecay (prehadronization) region where due to  $q\bar{q}$  pair creation the string tension is attenuated at separations  $r \geq R_1 = 1.2 \text{ fm} - 1.4 \text{ fm}$ .

In this physical picture it is important to take into account the specific character of the  $\pi$ -meson interaction with a light quark which occurs at the end of the string and therefore the string does not break due to the  $\pi$ -meson emission and this fact reconciles a high probability of pionic exchanges for the mesons with the existence of linear Regge trajectories.

The explicit and very simple model of the modified confining potential where the string tension depends on the separation  $r$  for  $r \geq R_1$ , allows to obtain the masses of the radicals in good agreement with experiment and may be considered as an explanation for the observation that the masses of high excitations are lowered. In particular the centers of gravity of the  $2P_J$  and  $3P_J$  multiplets appear to be lower by  $\simeq 200$  MeV and  $\simeq 350$  MeV respectively. The slope of the  $n_r$ -trajectory  $\Omega$  ( $L \neq 0$ ) is found to be 1.35- 1.22 GeV<sup>2</sup> in agreement with the analysis in Ref.[3]. For the  $nS$  states the calculated slope is found to be larger,  $\Omega \sim 1.5$  GeV<sup>2</sup>. The mechanism of reduced string tension has a universal character and does not depend on the quantum numbers and concrete positions of open thresholds in meson decays.

The authors would like to express their gratitude to the theory group of Thomas Jefferson National Accelerator Facility (TJNAF) for their hospitality. One of the authors (Yu.A.S.) was supported by DOE contract DE-AC05-84ER40150 under which SURA operates the TJNAF. This work was partly supported by the RFFI grant 00-02-17836 and INTAS grant 00-00110.

## APPENDIX A: MATRIX ELEMENTS FOR THE SOLUTIONS USING THE MODIFIED LINEAR POTENTIAL

Here we present some characteristics of the SSE solutions Eq. (2.2) for the modified confining potential Eq. (4.1) needed to calculate the spin-averaged meson masses. The eigenvalues of the Eq. (2.2) for the potential Eq. (4.1) plus Coulomb potential with parameters Eq. (4.4) and  $\sigma_0 = 0.19$  GeV<sup>2</sup> are given in Table IX for the  $S$ - and  $P$ -wave mesons ( $\alpha_s = 0.30$ ), and in Table X for the  $D$ - and  $F$ -mesons ( $\alpha_s = 0.21$ ).

We give also the constituent masses and the matrix elements  $\langle r^{-1} \rangle$  entering the string corrections  $\Delta_{\text{str}}(nL)$  and  $\Delta_{\text{SE}}(nL)$  while the average values of  $\bar{\sigma} = \langle \sigma(r) \rangle_{nL}$  are given in Table II.

TABLE IX: The eigenvalues of the SSE Eq. (2.2) in GeV for the Coulomb plus modified confining potential Eq. (4.1) with the parameters Eq. (4.4),  $\sigma_0 = 0.19 \text{ GeV}^2$  and  $\alpha_s = 0.30$  ( $L \leq 4, n_r \leq 3$ )

$n_r \setminus L$	0	1	2	3	4
0	1.204	1.721	2.098	2.402	2.645
1	1.858	2.190	2.436	2.628	2.799
2	2.268	2.471	2.656	2.840	3.013
3	2.542	2.730	2.904	3.065	3.218

TABLE X: The constituent masses (in GeV) and the matrix elements  $\langle r^{-1} \rangle$  (in  $\text{GeV}^{-1}$ ) for the  $P$ - and  $D$ -waves for the same potential as in Table IX.

$n_r$	$1P$	$2P$	$3P$	$4P$
$\mu(nP)$	0.464	0.484	0.535	0.587
$\langle r^{-1} \rangle$	0.250	0.203	0.180	0.168
	$1D$	$2D$	$3D$	$4D$
$\mu(nD)$	0.526	0.527	0.529	0.620
$\langle r^{-1} \rangle$	0.186	0.137	0.134	0.135

We would like to note that for the modified confining potential the constituent mass grows by only about 15% for the  $D$ -wave states and about 25% for the  $P$ -wave states, in contrast to the situation for the standard linear potential (see Table III) where this growth is substantially larger. Also the matrix elements  $\langle r^{-1} \rangle$  for the  $nD$  states with  $n_r = 1, 2, 3$  turn out to be equal within 2%.

- 
- [1] Particle Data Group, Eur. Phys. J. C15 (2000) 1
- [2] A. Abele et al. (Crystal Barrel), Phys. Lett. B423 (1998) 175; C. Amsler, Rev. Mod. Phys. 70 (1998) 1293; P. Barnes, Talk on "Physics and Detectors for DAFNE", hep-ph/0001326; hep-ph/9907259
- [3] A.V. Anisovich, V.V. Anisovich, and A.V.Sarantsev, Phys. Rev. D62 (2000) 051502; V.V. Anisovich, hep-ph/0110326 and references therein
- [4] D.V. Bugg et al., Phys. Lett. B353(1995) 378; A.V. Anisovich et al., B471 (1999) 271; Nucl.

- Phys. A662 (2000) 319
- [5] S. Godfrey and N. Isgur, Phys. Rev. D32 (1985) 189; S. Godfrey, Phys. Rev. D31( 1985) 2375
  - [6] N. Isgur, R. Kokoski, and J. Paton, Phys. Rev. Lett. 54 (1985) 869; P. Barnes, F.E. Close, and E.S. Swanson, Phys. Rev. D52 (1995) 5242
  - [7] A.M. Badalian and B.L.G. Bakker, hep-ph/0202246
  - [8] Yu.A. Simonov, Phys. Atom. Nucl. 60 (1997) 2069; hep-ph/9704301; “QCD: Perturbative or Nonperturbative”, Proc. XVII Int. Sch. Phys., Lisbon, 29 Sept.- 4 Oct., 1999, p.60 (World Scien. 2000); hep-ph/9911237
  - [9] P. Geiger and N. Isgur, Phys. Rev. D41 (1990) 1595; *ibid.* D44 (1991) 799; Phys. Rev. Lett. 67 (1991) 1066; Phys. Rev. D47 (1993) 5050
  - [10] N. Isgur, Phys. Rev. D60 (1999) 054013
  - [11] A.M. Badalian et al., Phys. Rep. 82 (1982) 31
  - [12] Yu.A. Simonov, to be published in Phys. Rev. D; hep-ph/0201170
  - [13] U. Glassner et al., Phys. Lett. B383 (1996) 98; hep-lat/9604014; K. Schilling et al., Nucl. Phys. proc. Suppl. 83 (2000) 140; hep-lat/9909152 ; B. Bolder et al., Phys. Rev. D63 (2001) 074504; hep-lat/0005018
  - [14] A. Duncan, E. Eichten, and H. Thacker, Phys. Rev. D63 (2001) 111501; hep-lat/0011076
  - [15] A. DiGiacomo and H. Panagopoulos, Phys. Rev. B285 (1992) 133; M. D’Elia, A. DiGiacomo, and E. Maggiolaro, Phys. Lett. B408 (1997) 315; G.S. Bali, N.Brambilla, and A.Vairo, Phys. Lett. B421 (1998) 265; hep-lat/9709079
  - [16] V.L. Morgunov, A. Nefediev, and Yu.A. Simonov, Phys. Lett. B459 (1999) 653; hep-ph/9906318
  - [17] Yu.A. Simonov, Phys. Lett. B515 (2001) 137; hep-ph/0105141
  - [18] A.Yu. Dubin, A.B. Kaidalov, and Yu.A. Simonov, Phys. Lett. B323 (1994) 41; *ibid.* B343 (1995) 310
  - [19] C.R. Allton et al., Phys. Rev. D65 (2002) 054502; hep-lat/0107021
  - [20] C. Bernard et al., Phys. Rev. D62 (2000) 034503; hep-lat/0002028
  - [21] Yu.A. Simonov, Z.Phys. C53 (1992) 419
  - [22] Yu.A. Simonov, Nucl. Phys. B307 (1988) 512; Phys. Atom. Nucl. 58 (1995) 309; hep-ph/9311216
  - [23] J. Schwinger, Phys. Rev. 82 (1951) 664; R.D. Ball, Phys. Rep. 182 (1989) 1; H.T. Sato, M.G.



Schmidt, and C. Zahlten, Nucl. Phys. B579 (2000) 492